Tellus (2006), 58A, 487–507

TELLUS

Seasonal climate forecasts of the South Asian monsoon using multiple coupled models

By TIRUVALAM N. KRISHNAMURTI[1]*, ASHIS K. MITRA[1,†], TALLAPRAGADA S. V. VIJAYA KUMAR[1], WONTAE T. YUN[1,‡] *and* WILLIAM K. DEWAR[2], [1]*Department of Meteorology, The Florida State University, Tallahassee, FL 32306-4520, USA;* [2]*Department of Oceanography, The Florida State University, Tallahassee, FL 23206-4320, USA*

(Manuscript received 15 November 2004; in final form 13 January 2006)

ABSTRACT

This study addresses seasonal climate forecasts using coupled atmosphere–ocean multimodels. Using as many as 67 different seasonal-forecast runs per season from a variety of coupled (atmosphere–ocean) models consensus seasonal forecasts have been prepared from about 4500 experiments. These include the European Center's DEMETER (Development of a European Multi-Model Ensemble System for Seasonal to Inter-Annual Prediction) database and a suite of Florida State University (FSU) models (based on different combinations of physical parametrizations). This is one of the largest databases on coupled models. The monsoon region was selected to examine the predictability issue. The methodology involves construction of seasonal anomalies of all model forecasts for a number of variables including precipitation, 850 hPa winds, 2-m/surface temperatures, and sea surface temperatures. This study explores the skills of the ensemble mean and the FSU multimodel superensemble. The metrics for forecast evaluation include computation of hindcast and verification anomalies from model/observed climatology, time-series of specific climate indices, and standard deterministic ensemble mean scores such as anomaly correlation coefficient and root mean square error. The results were deliberately prepared to match the metrics used by European DEMETER models. Invariably in all modes of evaluation, the results from the FSU multimodel superensemble demonstrate greater skill for most of the variables tested here than those obtained in earlier studies. The specific inquiry of this study was on this question: is it going to be wetter or drier, warmer or colder than the long-term recent climatology of the monsoon; and where and when during the next season? These results are most encouraging, and they suggest that this vast database and the superensemble methodology are able to provide some useful answers to the seasonal monsoon forecast issue compared to the use of single climate models or from the conventional ensemble averaging.

1. Introduction

In recent years, a number of papers have addressed seasonal forecasts of the Asian monsoon. These studies have examined impacts from a range of parameters such as the role of land surface processes, soil moisture and sea surface temperatures (SSTs) anomalies on interannual variability. Shen et al. (1998), Douville et al. (2001) and Douville (2002) addressed soil moisture impacts, and Molteni et al. (2003) addressed impacts of SST anomalies. Most of these studies utilized atmospheric general circulation models (AGCM; a list of acronyms is presented in Table 1) where the SST anomalies and sea ice were prescribed. The important message from these studies was a clear sensitivity of the Asian summer monsoon to the lower boundary physics such as land surface processes, soil moisture and SST anomalies, especially over the equatorial Pacific and the Indian Ocean. Slingo and Annamalai (2000) looked at the response of the Indian summer monsoon to the major El Niño SST anomalies of the year 1997. They also compared their results with another major El Niño event of 1982. They noted that strong El Niño does not always affect the Indian monsoon rainfall in the same manner. The monsoon of 1982 was very deficient in rainfall, whereas the monsoon of 1997 encountered heavier than normal rains. They attributed such differences to the manner of excitation of the Hadley and Walker circulations. They noted that the Walker circulation responses for the two contrasting years were affected by the latitudinal location of the rising branch of the Hadley circulation. Those were the factors other than the

*Corresponding author.
e-mail: tnk@io.met.fsu.edu

†Permanent affiliation: National Centre for Medium Range Weather Forecasting, Noida, UP-201307, India.
‡Permanent affiliation: Korea Meteorological Administration, Seoul, PIN-156720, S. Korea.
DOI: 10.1111/j.1600-0870.2006.00184.x

Table 1. List of Acronyms

AGCM	Atmospheric General Circulation Model
AMIP	Atmospheric Model Intercomparison Project
CERFACS	Centre Européen de Recherche et de Formation Avancée en Calcul Scientifique
DEMETER	Development of a European Multimodel Ensemble system for seasonal to inTERannual prediction
DMSP	Defense Meteorological Satellite Program
ECMWF	European Centre for Medium-Range Weather Forecasts
EM	Ensemble Mean
EOF	Empirical Orthogonal Functions
EQUINOO	Equatorial Indian Ocean Oscillation
FSU	Florida State University
FSUCGCM	FSU Coupled Ocean–atmosphere General Circulation Model
INGV	Istituto Nazionale di Geofisica e Vulcanologia
IOD	Indian Ocean Diplole
ISO	Intra Seasonal Oscillation
LODYC	Laboratoire d'Océanographie Dynamique et de Climatologie
MJO	Madden–Julian Oscillation
MPI	Max Planck Institute
NASA	National Aeronautics And Space Administration
OLR	Outgoing Longwave Radiation
PC	Principal Component
RMS Error	Root Mean Square Error
SEM	Ensemble Mean of Synthetic Data Set
SSF (or SSE)	Synthetic Superensemble Forecasts
SSM/I	Special Sensor Microwave/Imager
SST	Sea Surface Temperature
SSTA	SST Anomaly
TRMM	Tropical Rainfall Measuring Mission
UKMO	United Kingdom Met Office

equatorial Pacific SST anomalies. Indian Ocean SST anomalies and the Indian Ocean dipole phenomena in particular can modulate the local Hadley circulation and the associated monsoon rainfall (Behera et al., 1999; Ashok et al., 2001, 2004).

Multimodel based ensemble and superensemble forecasts of the monsoon have been addressed by Krishnamurti et al. (2000a), Wang et al. (2004), Kang et al. (2002), Wu et al. (2002) and Krishnamurti and Kumar (2004). Several of these studies were based on AGCM with prescribed lower boundary conditions. The coupled model based studies, such as Fu et al. (2002) and Krishnamurti et al. (2003), concluded that these coupled simulations are promising for better prediction of the Madden–Julian Oscillations (MJO) and hence of the intraseasonal oscillations that have a large control on the monsoonal dry and wet spells. The use of multimodel ensemble mean has shown some improvement in monsoon forecasts over those of single models. The FSU superensemble appears to do better than an ensemble mean because it deploys weights (for combining models) that are based on past performance and vary three-dimensionally for each model and for each variable at each geographical and vertical coordinates. By deploying as many as 10^7 weights for the training phase, it seems to reduce RMS error of the forecasts.

Some of our earlier research applications on seasonal climate forecasts involved the AMIP1 and AMIP2 global multimodel climate data sets covering long integration over a period of decade each using atmospheric general circulation models (Gates et al., 1999). These models share the same fields of SST and sea ice. The models are quite diverse in their structure, resolution, and physical parametrizations. These integrations were produced by a global community of modellers. The data sets for these experiments were managed by the Lawrence Livermore Laboratory in California. In a recent study, Krishnamurti et al. (2000a) selected some 13 models of AMIP1 to examine the monsoon forecasts based on the detailed evaluation of these data sets by Gadgil and Sajani (1998). A string of 8 yr of forecasts was used to develop the training phase and it was noted that individual models show considerable variability in skill, and the results from the superensemble reduced the meridional wind RMS error from 3 to 4 m s^{-1} to the level of 1 m s^{-1} consistently. Such improved results from the conventional superensemble were noted for many variables (Krishnamurti et al., 2000a). A marked improvement in the forecasts of seasonal precipitation from the superensemble was also noted from these AMIP data sets. This AMIP exercise did not address how much improvement in rainfall anomalies (above those of climatology) was possible from the conventional superensemble. That is being addressed in the context of the multimodel suites of coupled atmosphere ocean models in this paper. Since the lower boundary parameters such as sea ice and SST are

explicitly predicted in coupled models, their skills in monsoon forecasts need to be compared with the AMIP type results.

A host of studies have addressed the monsoon predictability issues over seasonal time scales (Ji and Vernekar, 1997; Schubert and Wu, 2001; Sperber et al., 2001; and several others). All these studies note poor performance of forecasts in predicting Asian monsoon a season in advance. They attribute these difficulties to the large internal variability of the monsoon with somewhat less of a control for the local boundary forcings. In recent observational studies on monsoon seasonal climate, much emphasis has been placed on the combined roles of the Pacific and Indian Ocean SST anomalies (Anderson, 1999; Ashok et al., 2001; Gadgil et al., 2003; Ashok et al., 2004). Exploring the monsoon climate from coupled models is worthwhile to study the mutual interactions of the atmosphere and ocean over these different basins. A number of recent studies on the MJO/ISO simulations related to the monsoon climate have also emphasized the need for coupled models (Fu et al., 2002; Kemball et al., 2002; Inness and Slingo 2003). A purpose of the present study is to demonstrate that the use of multimodel superensemble (especially a variant called synthetic superensemble) using the coupled models can reduce the errors of seasonal climate forecasts somewhat. Given the current uncertainties of the model forecasts, we feel that this may be an avenue for future practical applicability.

This study at first examines the 'mean Asian summer monsoon' from the FSU global coupled model in terms of the low-level winds and the precipitation fields. Then the DEMETER and the FSU coupled model hindcasts were used separately to prepare the multimodel based seasonal climate forecasts for various fields. The multimodel ensembles were built in two stages. First, statistical correction is applied to each model's hindcast (precipitation and surface temperature), which was determined by regressing the leading PCs of simulated precipitation onto those of observed precipitation. This is called the 'synthetic database'. Second, a weighted average of the individual model statistically corrected hindcasts was made with the weights obtained by minimizing the mean square error of the combination over a training period called the 'Synthetic Superensemble'. It is shown that

Table 2. Details of the coupled models data used in this study

(a) Seven DEMETER Coupled Models Setup

	CERFACS France	ECMWF	INGV Italy	LODYC France	M-France	UKMO	MPI Germany
Atmos. Model	ARPEGE	IFS	ECHAM-4	IFS	ARPEGE	ARPEGE	ECHAM-5
Resolution	T63	T95	T42	T95	T63	2.5° × 3.75°	T42
	31 Levs	40 Levs	19 Levs	40 Levs	31 Levs	19 Levs	19 Levs
Atmos. IC	ERA-40	ERA-40	ERA-40	ERA-40	ERA-40	ERA-40	Coupled Run Relax to Obs sst
Ocean Model	OPA 8.2	HOPE-E	OPA 8.1	OPA 8.2	OPA 8.0	GloSea OGCM Had CM3 based	MPI-OMI
Resolution	2° × 2°	1.4° × 0.3°–1.4°	2° × 0.5°–1.5°	2° × 2°	182 × 152 GP	1.25° × 0.3°–1.25°	2.5° × 0.5°–2.5°
	31 Levs	29 Levs	31 Levs	31 Levs	31 Levs	40 Levs	23 Levs
Ocean IC	Forced by ERA40	Forced by ERA40	Forced by ERA40	Forced by ERA40	Forced by ERA40	Forced by ERA40	Coupled Run Relax to Obs sst

(Further Details of the above coupled models can be found in Palmer et al., 2004.)

(b) Versions of the FSU Coupled Model Runs

	KOR	KNR	AOR	ANR
Atmos. Model	FSUGSM	FSUGSM	FSUGSM	FSUGSM
Resolution	T63/14 Levs	T63/14 Levs	T63/14 Levs	T63/14 Levs
Atmos. IC	ECMWF with Phy. Init	ECMWF with Phy. Init	ECMWF with Phy. Init	ECMWF with Phy. Init
Atmos. Physics	Kuo	Kuo	SAS	SAS
	Radiation Old (Emissivity/ Absorbtivity Based)	Radiation New (Band Model)	Radiation Old (Emissivity/ Absorbtivity Based)	Radiation New (Band Model)
Ocean Model	HOPE Global	HOPEGlobal Global	HOPEGlobal Global	HOPEGlobal Global
Resolution	5° × 0.5°–5°	5° × 0.5°–5°	5° × 0.5°–5°	5° × 0.5°–5°
	17 Levs	17 Levs	17 Levs	17 Levs
Ocean IC	Coupled Assimilation Relax Obs SST	Coupled Assimilation Relax Obs SST	Coupled Assimilation Relax Obs SST	Coupled Assimilation Relax Obs SST

the multimodel forecasts are better than the simple ensemble mean.

2. Models/data sets

Two sets of data from coupled models are used in the present study and are described below.

2.1. DEMETER models

These models are described in Palmer et al. (2004). The following is a list of European Coupled Seasonal Climate Models that fall in this category: (1) Three coupled models from France (CERFACS, LODYC, METEO FRANCE) (2) the ECMWF Coupled model (3) the UK Met office Coupled model (4) an Italian model INGV and (5) a model from Germany (MPI). Each seasonal forecast had a 1 month lead time. Data from 4 month forecasts were selected for each initial condition, covering the years 1987–2001. These seven coupled models carried an ensemble of nine forecasts each for each start date. Those ensembles were constructed using wind and SST perturbations on the respective initial conditions. In all some 3780 seasonal forecasts were available from the DEMETER database. An initial ensemble mean of these nine-member forecasts was performed to reduce the number of total DEMETER forecasts to seven members. Table 2a describes some features of these coupled models.

2.2. FSU suite of coupled models

These four identical models share the same initial coupled data assimilation, resolution, dynamics, and most of the physical parametrizations except for the cumulus parametrization and the radiative transfer algorithms. This study uses two versions of the cumulus parametrization and two versions of radiative transfers following Krishnamurti et al. (2002) in the design of these FSU coupled models. These are summarized in the Table 2b. The relevant references for these algorithms for convection and radiation are Krishnamurti and Bedi (1988), Grell (1993), Chang (1979), and Lacis and Hansen (1974). The FSU coupled model combines the FSU global spectral model (Krishnamurti et al., 1998) and the Hamburg Ocean model (Latif, 1987). A schematic outline of the FSU coupled model strategy is described in Fig. 1. The model's performance is described in Krishnamurti et al. (2002). The model experiments contain the following two components in its data assimilation. (1) An ocean spin up component: Using monthly mean surface winds from the ECMWF reanalysis and the Reynold's SST fields, we first spin up the ocean with the ocean model alone. Here Newtonian relaxation of the observed SST and imposed wind stresses drives the ocean for all the 11 yr period. Details of this procedure are presented in LaRow and Krishnamurti (1998) and Krishnamurti et al. (2000b). (2) Coupled assimilation: A coupled assimilation phase utilizes the FSU coupled model, where a physical initialization following Krishnamurti et al. (1991) and a Newtonian relaxation assimilate the atmospheric and oceanic data sets. Here the observed rain rates used in the physical initialization are derived from DMSP/SSMI based on microwave scattering temperatures and the NASA TRMM satellites. This assimilation also includes a Newtonian relaxation for the observed SSTs. This is all done with daily rainfall and weekly Reynold's SST data sets. In this process, the model based daily rainfall totals are brought to a

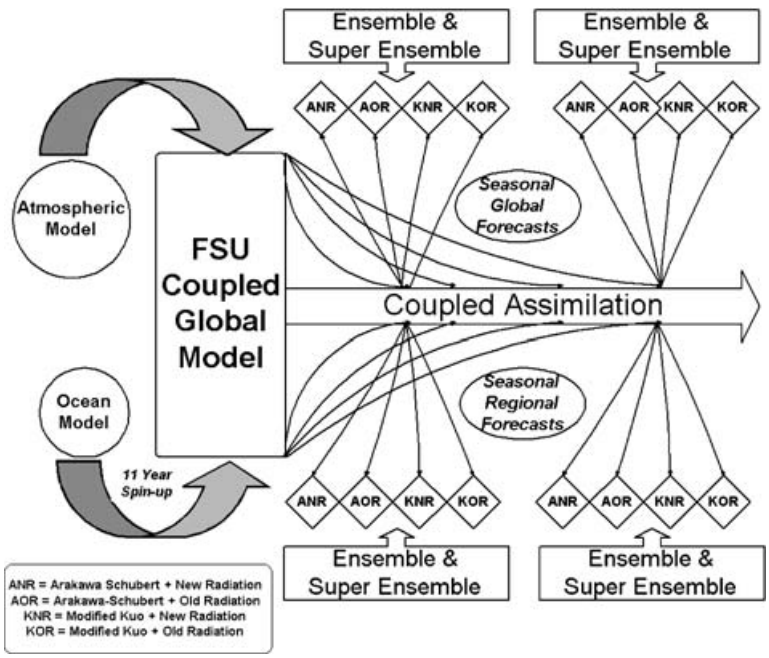

Fig. 1. A Schematic outline of the FSU Coupled model Strategy. It includes features such as ocean spin up, coupled assimilation and ensemble member forecasts.

close agreement with observed (analysis) precipitation at the same resolution. This assimilation tries to retain the temperature of air and the rotational parts of the winds of the ECMWF's daily analysis using a hard nudging, while permitting the divergent part of the wind, the surface temperatures; the humidity fields and the convective heating profiles to evolve with a soft nudging. The choices of relaxation coefficients for the nudging are presented in Krishnamurti et al. (2002).

Using the aforementioned four versions of the coupled model, we carried out about 720 experiments, one experiment per month, over the period 1987–2001. Data sets of wind components, air temperatures, humidity, pressures, geopotential heights, precipitation, surface fluxes, and components of diabatic heating, SST, subsurface temperature, and salinity over global oceans and the ocean currents were archived for all forecasts starting at intervals of every 15 days. Combining the DEMETER and the FSU components, a total of 11 global coupled ocean–atmosphere models provided data sets for a total of 4500 seasonal forecast experiments.

3. Mean monsoon in the FSUCGCM

3.1. Simulation of the wind field and precipitation

In the validation of any climate model, it is important that the current climates from the model and from observation/analysis are carefully compared. In this section, we focus on the quality of simulations for the Asian monsoon region by the 'Florida State University Coupled Ocean–atmosphere General Circulation Model' (FSUCGCM) for the summer monsoon season. The predictability and the interannual variability of Asian summer monsoon rainfall in a model are dependent on how well that model simulates the climatological mean monsoon (Sperber and Palmer, 1996). Models with better rainfall climatology generally have less systematic errors and can have somewhat higher ability to simulate interannual variations. Climate drift is almost inevitable in coupled ocean–atmosphere models. Oftentimes the climate drift can be larger than the interannual signal. This section explains the model climate and any possible drifts. The mean features of summer monsoon and its variability, produced by the FSUCGCM seasonal forecasts were investigated for the period 1987–2001. Lower level wind flow patterns and rainfall associated with the summer monsoon season were examined. The observation based mean fields were compared with simulated fields by this coupled model for June, July and August (JJA) period. The overall spatial low-level wind flow patterns and the precipitation distributions over the Indian continent and adjacent oceanic regions were comparable to the respective monthly mean and seasonal mean analyses. In this sense, the coupled model was able to capture the large-scale features of monsoon circulation and the associated rainfall quite reasonably. Some of these fields are illustrated in this section.

The observed winds (from ECMWF 40 yr reanalysis) and the seasonal climatological forecast errors for the 850 hPa level winds for months 1, 2 and 3 of forecasts are shown in Fig. 2. These are the 15 yr climatology (1987–2001) of the summer months June–August. The forecast results are for the ensemble mean of the four FSU models. These clearly show that the FSU model ensemble mean underestimates the amplitude of the entire gyre from the cross-equatorial flow to the southwesterly flows of the monsoon. The ensemble mean has an easterly bias of the order of 2 to 4 m s^{-1}. The RMS errors of the 850 hPa winds are around 4.2, 4.6 and 4.5 m s^{-1} for the three respective months over this monsoon domain. The superensemble corrects this type of a systematic error, which is the main topic of this study.

Figure 3a shows the observed mean rainfall for the Northern Hemisphere summer season June-August of 1987–2001. The heaviest rainfall occurs over the northern Bay of Bengal (>15 mm day^{-1}). The other centres with large values are found over the west coastal and offshore area of India. The mean forecast

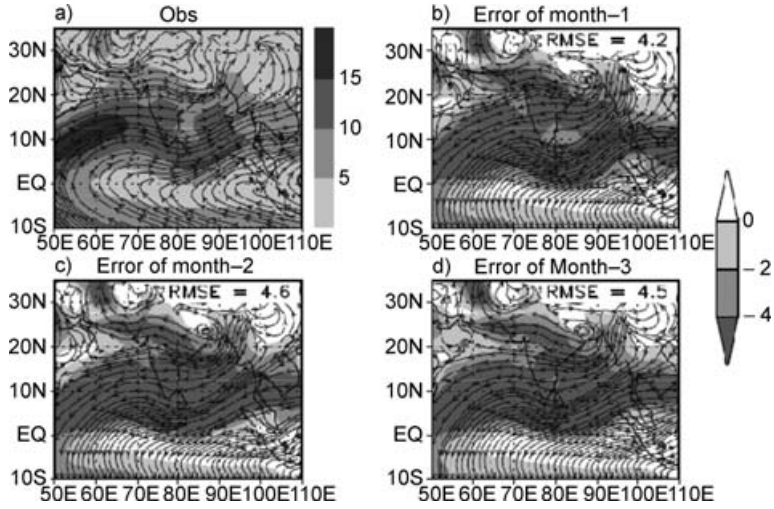

Fig. 2. Climatology (1987–2001) of observed (ERA-40) and predicted (ensemble mean of four FSU coupled models) wind field at 850 hPa during June-August: a) observed wind speed (shaded; m s^{-1}) and stream function; b–d) errors of wind speed (shaded; m s^{-1}) and stream function for months 1, 2 and 3 of forecasts. The RMS error of the wind speed over this domain is indicated as numbers inside the forecast panels.

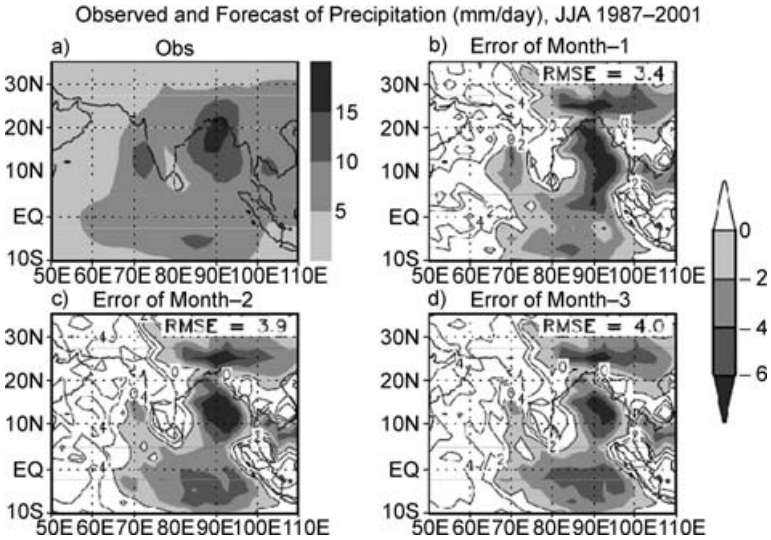

Fig. 3. Same as Figure 2 but for the precipitation climatology (mm day^{-1}). The observed rain was obtained from the CMAP (Xie and Arkin 1997) data sets.

error distribution during this period (for the ensemble mean) of the FSU models is shown in Figs. 3b–d. In all these forecasts the heaviest total rain is underestimated by almost 4 mm day^{-1} mainly over the Bay of Bengal and over the eastern Equatorial Indian Ocean. The error distributions are roughly between ±4 mm day^{-1}. The RMS errors of forecast of the seasonal totals increase from 3.4 to 3.9 to 4.0 mm day^{-1} during the months 1, 2 and 3 of forecasts, respectively. Model climatology based on month 1 through month 3 of forecasts did not show any drift or inconsistencies in general. Over the southeastern part of India, the model has a slight tendency to over predict by 10% the monsoon rainfall from its month 1 through month 3 of climatology.

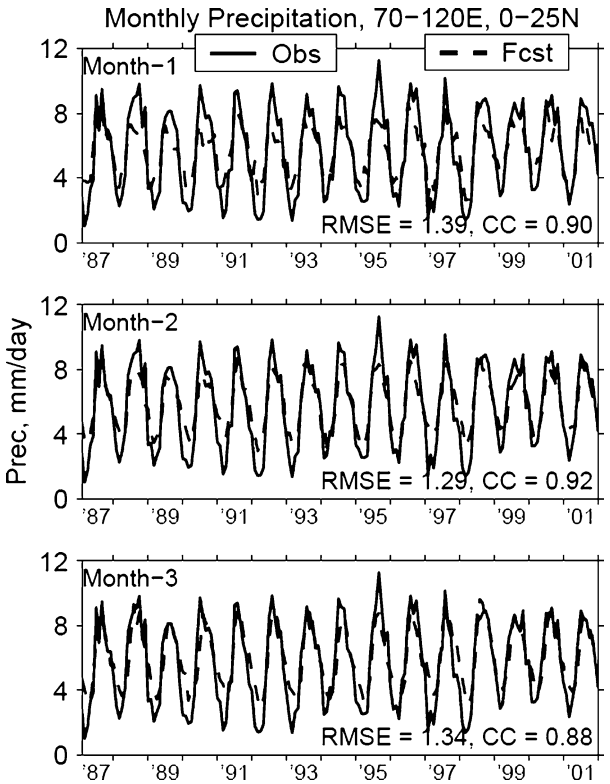

Fig. 4. Monthly values of precipitation based on Xie and Arkin (1997) data sets and those from the FSU four-model ensemble mean showing the seasonal cycle over 16 yr (Indian monsoon region, 70°–120°E and 0°–25°N). The solid lines are from observations and the dashed lines are based on strings of months 1, 2 and 3 of forecasts. Units are in mm day^{-1}.

The total rainfall over the South Asian monsoon region (70°–120°E; 0°–25°N) from the ensemble mean of four FSU models is shown in Fig. 4. This figure presents the total precipitation for the months 1, 2 and 3 of forecasts. This covers each month for the year 1987 through 2001. Although the phase of the ensemble mean is quite accurate, the amplitude of the predicted ensemble means is slightly less than the observed monthly means. The monthly RMS errors and the anomaly correlations of the forecasts are shown inside each panel. They show that the best results were obtained for month 2 of the forecasts suggesting a spin up of the FSU models. These results are somewhat improved from the use of the FSU superensemble which is the main topic of this paper.

A relative comparison of the observed climatological rainfall totals and model based rainfall totals for the summer months June–August for the year 1987–2001 are shown in Fig. 5. The panel 'a' shows the observed climatological totals in mm day^{-1}. Panels 'b' through 'h' show the results from a number of European coupled climate models and panel 'i' shows results of total rains for the ensemble mean from the suite of 4 FSU models. Among the different models shown here, the LODYC and the UKMO models simulated the Bay of Bengal and the Arabian Sea features, although the later predicted extensive rain inland north of the Bay of Bengal. Both of these models fail to simulate the precipitation maxima over southern Indochina. The FSU model appears to have reasonable rainfall climatology for the

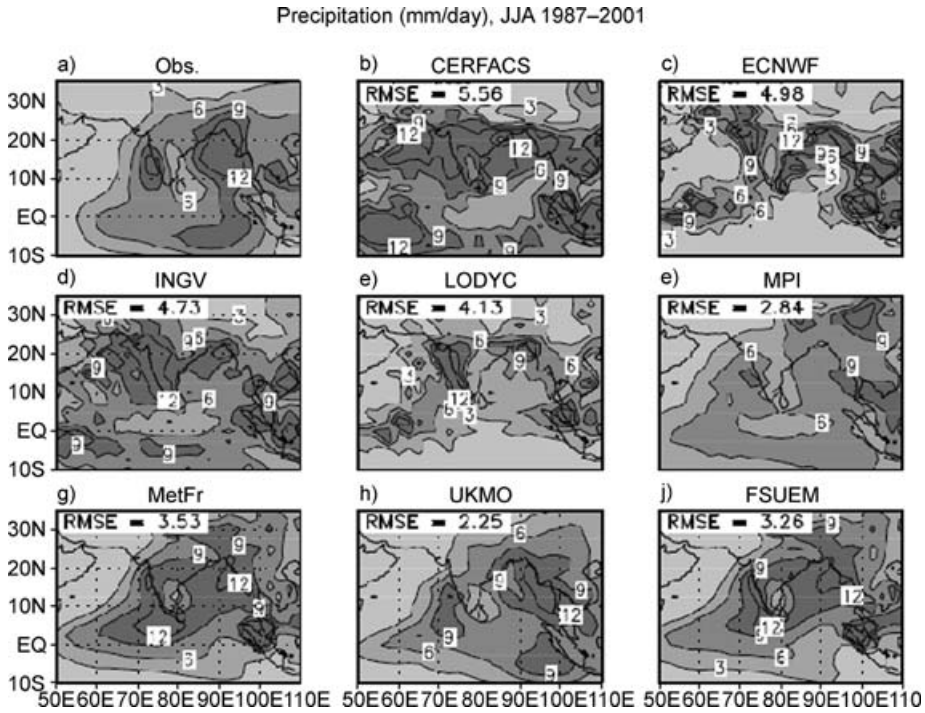

Fig. 5. Observed and model climatology of seasonal precipitation (June–July–August). Observed is shown on top left. The bottom right shows the FSU 4 model ensemble mean. The remaining panels carry the DEMETER member models (their ensemble mean). Units are in mm day^{-1}. Mean is for the period from 1987 to 2001.

summer monsoon, although there are some minor phase shifts in the overall features. Most other models are unable to capture the rainfall maxima near the head Bay of Bengal and the west coast mountain regions of the monsoon system. The RMS errors (shown as numbers inside the panels) of the model forecasts range from 2.25 mm day^{-1} for the U.K. Met Office model to 5.56 mm day^{-1} for the CERFACS model. Those for the FSU ensemble mean were around 3.26 mm day^{-1}.

3.2. SST Simulations and their impacts on the monsoon

Numerous observational studies have addressed the impacts on the Indian monsoon rainfall from the El Niño and the Indian Ocean Dipole (Rasmussen and Carpenter, 1983; Anderson, 1999; Barnett, 1983; Behera et al., 1999; Murtugudde et al., 2000; Rao et al., 2002; Saji et al., 1999; Webster et al., 1999; Vinayachandran et al., 2002; Lau and Nath, 2003, 2004; Rao et al., 2004). Often an El Niño year is associated with below normal monsoon rainfall over India. El Niño frequency is once in roughly 4–6 years. Another important feature is the Indian Ocean Dipole, which is an east-west seesaw of convection and OLR over the near-equatorial Indian Ocean. These two centres of action are located near 60°E and 100°E, respectively. From an analysis of over 100 yr of rainfall and its relationships to El Niño, it was seen that in only over 50 % of the years, the well-known inverse relationship between the equatorial Pacific SST anomaly and the Indian monsoon rainfall has been noted. The Indian Ocean Dipole appears to be another important contributor to the monsoon rainfall anomalies (Ashok et al., 2001; Gadgil et al., 2003).

The influence of the Indian Ocean Dipole is subtler; when the western lobe of the dipole is more active with convection, Indian monsoon rainfall activity tends to be above normal and the converse is the case for the western lobe. Gadgil et al. (2003) have arrived at a lower tropospheric wind index that is also related to this dipole, called EQUINO. Southern trades over the near equatorial Indian Ocean are somewhat weaker during seasons of above normal Indian monsoon rainfall activity. The converse is the case during the opposite phase of this dipole. By combining this wind index and the southern oscillation index, Gadgil arrived at a measure that appeared to carry a very high degree of skill for the nowcasting of Indian monsoon rainfall from a combined index where the influence of the two ocean basins is considered. Both the western and eastern poles of the IOD influence the ENSO impact on the monsoon, and this phenomenon was studied extensively by Ashok et al. (2004) using a series of AGCM experiments. The results of these experiments qualitatively support Gadgil et al. (2003) work discussed above. In the context of the coupled model results from the synthetic superensemble, we can examine some of our results of forecasts in order to enquire whether or not the model carries some reasonable fidelity of these measures.

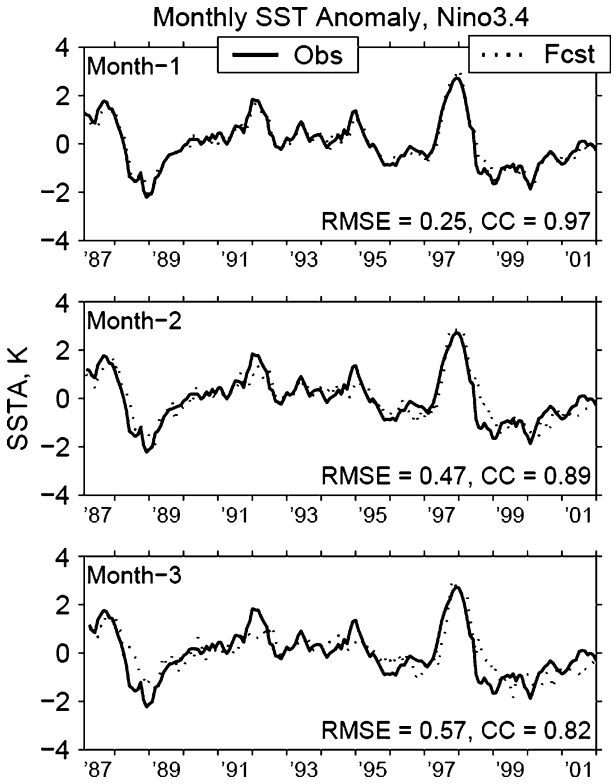

Fig. 6. Observed (solid) and month-by-month forecasts (dotted) of SST anomaly (in K) over the Niño 3.4 region. The three panels show forecast at the end of months 1, 2 and 3.

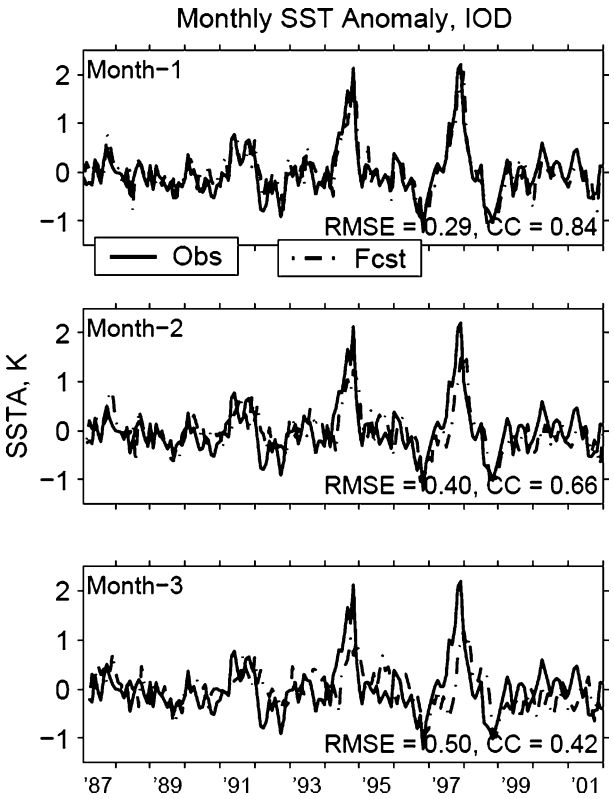

Fig. 7. Observed (solid) and month by month forecasts (dashed-dot line) of SST anomaly difference (in K) between the western and eastern Indian Ocean (related to Indian Ocean dipole). The three panels show forecasts at the end of months 1, 2 and 3.

Figures 6 and 7 contain several graphs, based on observed and coupled model-based forecasts that illustrate the El Niño and Indian Ocean Dipole SSTA simulations. These are the ensemble mean forecasts based on the suite of four FSU models. The observed SST anomalies for the Niño 3.4 region are plotted along with the forecasts (at end of the months 1, 2 and 3). These are very closely predicted for month 2 of the forecasts. The RMS errors and the anomaly correlations of the time series for months 1, 2 and 3 of forecasts are indicated within the respective panels of the figure. The RMS errors increase as the lead time of the forecast increases (0.25 K for month 1, 0.47 K for month 2 and 0.57 K for month 3). The anomaly correlations carry a value as high as 0.97 for month 1 of forecasts and reduce to 0.89 and 0.82 for months 2 and 3 of forecasts. Moreover, forecast of SSTA for months 2 and 3 shows the growth of small phase errors. Overall, the FSU model is able to capture the entire essential SSTA variability very reasonably over an entire season for several cycles of the El-Nino occurrences. A realistic handling of the SST anomaly in the west Pacific and the Indian Ocean region are a prerequisite for the monsoon rainfall simulations. Such realistic agreement of the observed and the modelled rainfall variability was illustrated in Fig. 4 for the monsoon region, where we noted the essential variability of the total monsoon rainfall over India being well captured. Compared to the performance of the individual member models, the ensemble mean appears to illustrate the total rainfall variability very well. The simulation of the Indian Ocean Dipole is illustrated from a plot (Fig. 7) of the difference in SST between the western and the eastern designated regions. Here again we compare the plots of the observed and the ensemble mean based forecast differences. It is clear that in these two to four month forecasts the model is able to capture the seesaw of the dipole behaviour in the SST anomalies. A reasonable high skill for month 1 of forecasts for the RMS error and anomaly correlation (0.29 K and 0.84, respectively) can be noticed. For months 2 and 3, these skills are 0.40 K and 0.66, and 0.50 K and 0.42, respectively. Of special interest for seasonal monsoon forecasts are the SSTA over the Niño region (Fig. 6) of the equatorial Pacific Ocean and the near equatorial dipole seesaw of the Indian Ocean (Fig. 7). The interannual variability of those features was handled well by the FSU model.

4. Multimodel ensemble forecasts

4.1. Conventional superensemble methodology

The superensemble technique (Krishnamurti et al., 1999) produces a single forecast derived from a multimodel set of

forecasts. Forecasts from this methodology do carry the highest skill compared to participating member models of the ensemble, and they carry skills above those of the bias-removed ensemble mean representation. The strategy for the multimodel superensemble partitions the forecast time line into two components. The first of these, called the training phase, utilizes the multimodel forecasts and the observed (analysis) fields to derive model performance statistics. The second phase, called 'the forecast phase', utilizes the multimodel forecasts and the aforementioned statistics to obtain superensemble forecasts into future. During training, with the use of benchmark observed (analysis) fields, past forecasts are used to derive statistics on the past behaviour of the models. Given a set of past multimodel forecasts, we have used a multiple regression technique (for the multimodels), in which the model forecasts were regressed against an observed (analysis) field. This utilizes a least squares minimization of the difference between anomalies of the model and the analysis fields in order to determine a distribution of weights. These regression coefficients associated with each individual model conceivably can be interpreted as a measure of that model's relative reliability for the given point over the training period. For each model prognostic variable, the purpose of training is to evaluate model biases geographically and vertically. This being done for $\boldsymbol{m}$ multimodels at $\boldsymbol{n}$ grid points (along the horizontal and vertical) for $\boldsymbol{p}$ variables and $\boldsymbol{q}$ time intervals constituted as many as $\boldsymbol{m}*\boldsymbol{n}*\boldsymbol{p}*\boldsymbol{q}$ statistical coefficients (which came to around 10^7 weights). This degree of detail for the construction of the superensemble was found necessary. The methodology for this conventional procedure consists of a definition of the superensemble forecast:

$$S = \overline{O} + \sum_{i=1}^{N} a_i (F_i - \overline{F}_i) \ldots, \tag{1}$$

where S is the superensemble prediction, $\overline{O}$ is the observed time mean, a_i are the weights for individual models i, F_i is the predicted value from model i, $\overline{F_i}$ is the time mean of prediction by model i for training period, and N is number of models. The weights are computed at each of the grid points by minimizing the objective function $\boldsymbol{G}$ for the mean square error of the forecasts:

$$G = \sum_{t=0}^{t=\text{train}} (S_t - O_t)^2 \ldots, \tag{2}$$

where 't' denotes the length of a training period.

In this conventional superensemble methodology a collection of a sequence of individual forecasts from several models are subjected to a multiple regression against the observed (or assimilated) counterpart fields. These multiregression coefficients are collected for a training phase of the superensemble. The length of this training data phase varies for each type of forecast addressed in this paper. These statistics, collected during the training phase are simply passed on to a forecast phase of the superensemble. In this forecast phase, we again have forecasts, from the same member models, that are corrected for their past collective behaviour. This type of local bias removal is more effective compared to a conventional bias removed ensemble mean. The later assigns a weight of 1.0 to all models after bias removal. The superensemble includes fractional and even negative weights depending on past behaviours. In a probabilistic sense also, the superensemble probability forecasts are somewhat better than the multimodel bias-removed ensemble at any threshold level (Stefanaova and Krishnamurti, 2002).

4.2. *Synthetic superensemble methodology*

A variant of the above conventional super ensemble formulation was necessary for improved skills for seasonal climate forecasts (Yun et al., 2005). From the member model forecast data sets, additional data sets named the 'Synthetic Data sets' were generated in this variant of the superensemble that contributed towards major improvements of the skills for seasonal climate forecasts. The synthetic data set is created from a combination of the past observations and past forecasts. A consistent spatial pattern is determined among the observations and forecasts. This is simply a linear regression problem in the EOF space. Sets of such synthetic forecasts are then obtained, one for each available forecast, for the creation of superensemble forecasts. The method of creating the synthetic data and the associated statistical procedure is described below.

The time series of observation can be written as a linear combination of EOFs such as,

$$O(x,t) = \sum_{n} P_n(t).\phi_n(x) \ldots, \tag{3}$$

where n is the number of modes selected. The two terms on the right hand side of above equation represents the time (principal component PC) and space (EOF) decomposition, respectively. PC time series $P(t)$ represents how EOFs (spatial patterns) evolve in time. PCs are independent of each other. Similarly the forecast data can be projected into the PCs and EOFs for i member models,

$$F_i(x,T) = \sum_{n} F_{i,n}(T).\varphi_{i,n}(x) \ldots. \tag{4}$$

Here index i represents a particular member model. i can vary from 1 to m. We are interested in knowing the spatial patterns of forecast data, which evolve in a consistent way with the EOFs of the observation for the time series considered. Here we use a regression relationship between the observation PC time series and a number of PC time series of forecast data,

$$P(t) = \sum_{n} \alpha_{i,n} F_{i,n}(t) + \varepsilon(t) \ldots. \tag{5}$$

In the above equation the observation time series $P(t)$ is expressed in terms of a linear combination of forecast time series $F(t)$ in EOF space. The regression coefficients α_n are found such that the residual error variance $\mathrm{E}(\varepsilon^2)$ is a minimum.

Once the regression coefficients are determined, the PC time series of synthetic data can be written as:

$$F_i^{reg}(T) = \sum_n \alpha_{i,n} F_{i,n}(T) \ldots . \quad (6)$$

Then the synthetic data set is reconstructed with EOFs and PCs as:

$$F_i^{syn}(x, T) = \sum_n F_{i,n}^{reg}(T).\phi_n(x) \ldots . \quad (7)$$

These synthetic data (m sets) generated from m member model's forecasts are now subjected to conventional FSU superensemble technique described earlier (Section 4a). Further details on the synthetic superensemble are described in Yun et al. (2005). The whole idea of this methodology is to filter out the components in the forecast that do not contain information about the future state of the climate, and to improve the forecasts by replacing biased versions of the patterns of variability contained in the forecasts with their observed counterparts. In the EOF construction, the global data was used always and the first 55 EOFs were utilized both for the observations and model forecasts. There was no marked improvement in results beyond these 55 EOFs. All the results pertaining to the skill scores discussed in the subsequent sections are from this 'Synthetic Superensemble' method described here.

5. Construction of the superensemble

It has been mentioned in Section 2 that two sets of seasonal forecasts from coupled atmosphere–ocean models were available for this study: the DEMETER set of models (seven in total) and the FSU set of models (4 in total). Monthly mean forecasts for 0 to 5 months in advance were available from both these suite of models during the years 1987–2001. However, in the construction of the superensemble for this study both these data sets were treated separately to calculate seasonal forecasts. The reason is that the use of three-monthly averaged data sets versus monthly data set to create the superensemble has an impact on skill scores. The DEMETER forecasts started at every 3 months (and forecasts are available for 0 to 5 months lead time). Therefore a single lead-time forecast was available for only at every 3 months in this data sets (e.g. 1-month lead time forecasts are available for March, June, September and December). Hence, a monthly time series with a constant lead time forecast was not possible to create for the DEMETER models. On the other hand, four FSU model data sets were available at lead times of 1, 2 and 3 months for every month of the calendar. This provides an opportunity to compare the skill of the superensemble created with monthly and seasonal mean data sets. A marked improvement in skill was noticed from the use of the continuum seasonal forecasts that are made every month as compared to the seasonal forecasts made every 3 months. Figure 8 shows such a result from the suite of FSU models. Here the superensemble was created in two different ways. In the first case the 1, 2 and 3 month lead time forecasts of the models were averaged to create four seasonal forecasts every year. This way there were 60 seasonal forecasts for the 15 yr. The superensemble forecast was created from this data sets using cross-validation technique (we will call it *3 month mean* superensemble). In the second case separate monthly time series were created for 1, 2 and 3 month lead-time forecasts, and three different superensemble forecasts were created using cross-validation technique for each of these time series. These superensemble forecasts are at 1, 2 and 3 month lead time. Now seasonal means were made from these forecasts (call it *month 123 mean* superensemble) to compare with the *3 month mean* superensemble created by the other method (described above). Figure 8 illustrates the improvement of RMS error (in mm day^{-1}) and anomaly correlation (open and shaded bars) over the South Asian monsoon region for the *month 123 mean* superensemble over the *3-month mean* superensemble during June-August of 1987–2001 and in the mean (denoted by *Mean*) of these years. An improvement of 0.1 to 0.3 for both RMS errors (in mm day^{-1}) and anomaly correlations can be noticed from this figure during most of the years of simulations. Another noteworthy feature of this result is that the ratio of the magnitude of the improvements for RMS errors and anomaly correlations during different years (except 1992) were roughly constant. In other words a higher improvement in RMS error was associated with a higher improvement in anomaly correlation and vice-versa. This shows that the overall forecast skill of the superensemble was improved using monthly mean forecast data

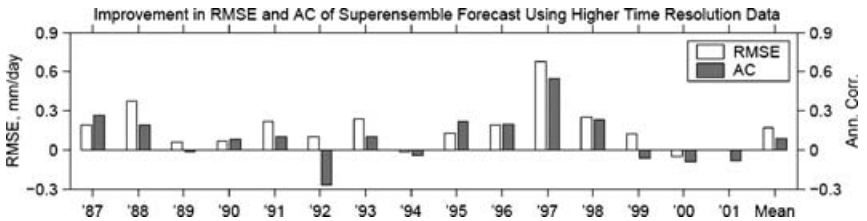

Fig. 8. Improvement in RMS error and anomaly correlation of synthetic superensemble forecast using monthly time series of forecasts as compared to seasonal mean time series of forecasts of the FSU models over the South Asian monsoon region (50°–110°E, 10°S–35°N) during June-August of 1987–2001 and on the average over these years (*Mean*). Note that, in general, a higher improvement in RMS error is associated with a higher improvement in anomaly correlation during most of the years of simulations.

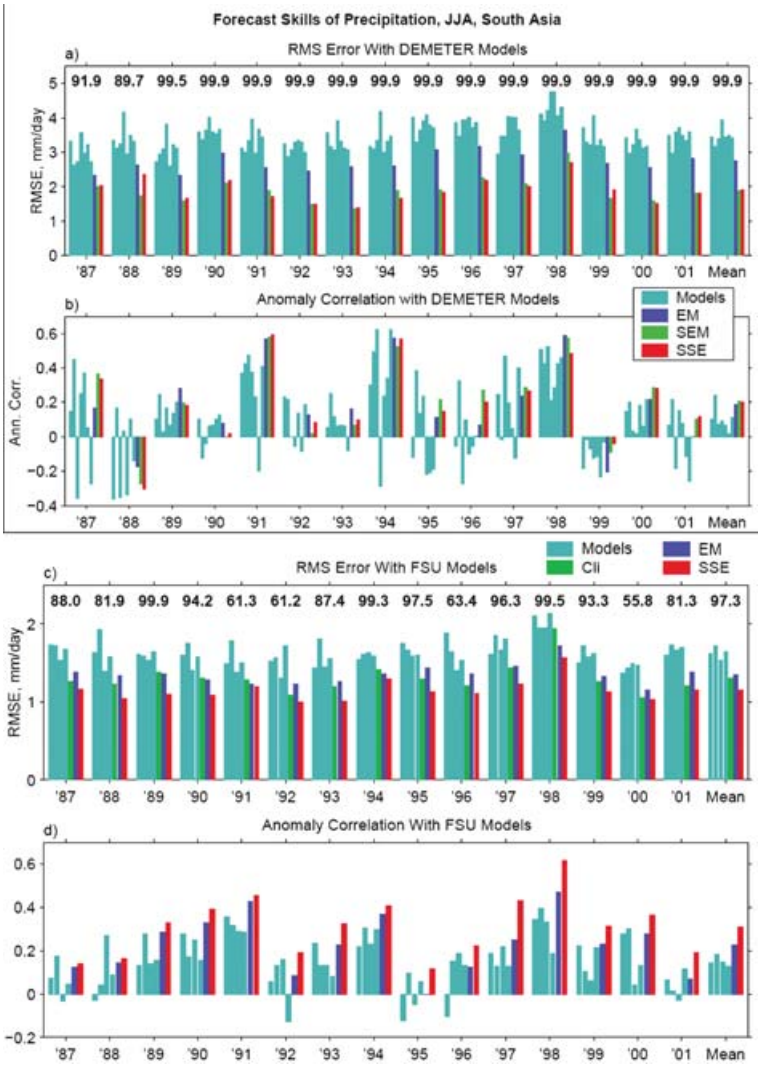

Fig. 9. Seasonal forecast skills of precipitation over the South Asian monsoon region (50°–110°E, 10°S–35°N) during June-August of 1987–2001: (a) RMS errors and (b) anomaly correlations for the suite of DEMETER models; c) RMS errors and d) anomaly correlations for the suite of FSU models. Legends: *Cli*: climatology; *EM*: ensemble mean; *SEM*: synthetic ensemble mean; *SSE*: synthetic superensemble; *Mean* in each panel denotes the mean of the parameter over the 15 yr of forecasts for this season. The confidence level at which the RMS error of the SSE was better than the RMS error of the ensemble mean is indicated (in percent) at the top of the panels against each year. The confidence level was calculated using a *t*-test.

as compared to seasonal mean forecast data of the same set of models.

6. Results and discussion

6.1. Precipitation forecast skills

This section addresses specific improvements in the skill of seasonal climate forecasts for individual seasons. Here the skills of member models, their ensemble mean, and the superensemble are compared. Figure 9 illustrates the error statistics (RMS errors and anomaly correlation) for seasonal forecasts of total precipitation covering the summer months (June, July and August). Figures 9(a) and (b) show the skills from DEMETER models and Figs. 9(c) and (d) show the skills from the FSU models for the precipitation forecasts over the South Asian monsoon domain extending from 50°–110°E and 10°S–35°N. These results are based on cross-validation, that is, all the years of forecasts, except for the one being addressed, are made a part of the training database successively. This was necessary since the data length was still quite small for the optimal development of a training phase (Krishnamurti et al., 2000a). Various bars in the skill score diagram indicate member models, ensemble mean (*EM*), ensemble mean of the synthetic data (*SEM*), the climatology (*Cli*) and the synthetic superensemble forecasts (*SSE*), respectively. Also shown, as numbers at the top of the panels against each years for the RMS errors, is the confidence level at which the SSE forecast is different compared to the EM forecast using a *t*-test. Results presented in these illustrations convey the same essential message, that is, a stepwise reduction of errors from the member models to the ensemble mean and finally to the best product, that is, the synthetic superensemble. The RMS errors for the member models are almost a factor of two larger than that of the synthetic superensemble. The right most groups of bars show the 15 yr summary of forecast improvements. Overall, the RMS errors are reduced considerably, since a reduction of RMS is a

built in feature for the design of our superensemble (eq. 7). This reduction was significant at more than 90% level for 14 out of the 15 yr of simulations for DEMETER models and for 7 out of the 15 yr of simulations for FSU models. And on the average (*Mean*), there were some improvements in the anomaly correlations (Figs. 9b and d), but not well marked. In principle, it is possible to design a superensemble for the improvement of the anomaly correlation in its own right. This is currently being explored to the design of a superensemble that can jointly reduce the RMS errors and enhance the anomaly correlation at the same time. This will be reported in a future publication.

The quality of forecasts from the ensemble mean and the superensemble are reasonable and match the high skills for the AMIP-based superensemble (Krishnamurti et al., 2000a). The AMIP seasonal precipitation forecast skills over the monsoon domain were quite high since they were based on specified observed lower boundary SST anomalies and sea ice. As stated previously, many authors have noted a lower skill for the seasonal forecasts of the monsoon. A premise that seasonal forecasts of the monsoon precipitation are influenced by internal dynamics, as contrasted from a boundary forcing, has been offered as a possible explanation for these lower skills. Since internal dynamics and boundary forcing are not mutually exclusive (i.e. one influences the other) in a non-linear system, such a partitioning of explanations is questionable. In a seasonal forecast a first month's boundary forcing can easily generate an internal (variability) dynamics for the next month. Thus, the reasons for poorer monsoon forecasts still are not quite apparent.

The monsoon precipitation forecast skills from the individual member models do reflect large RMS errors and a lower skill for the anomaly correlations. A marked reduction of the RMS errors from the synthetic superensemble and the synthetic ensemble mean was noted. These results are based on the DEMETER database; the suite of FSU coupled models and the combined suite of all models also show similar skill improvements from the synthetic superensemble. Improvements for the anomaly correlation skills are somewhat less compared to those for the RMS errors. In the following paragraphs the question as to how much improvement in the geographical distribution of seasonal total rainfall and the seasonal rainfall anomalies are obtainable from the use of the synthetic superensemble is addressed. It is also required to assess the improvement from the synthetic superensemble compared to those of the member models and that of the climatology.

Typical examples of the seasonal total rainfall forecasts over the monsoon region are illustrated in Fig. 10 from the FSU suite of models. All these forecasts use a lead time of 1 month. An average of these 3 months defines the seasonal rainfall forecast. This figure also shows the observed seasonal totals for JJA from the Xie and Arkin (1997) data sets. During 1991 and 1994, the synthetic superensemble projected a belt of above normal seasonal monsoon rainfall over Northern India, consistent with the

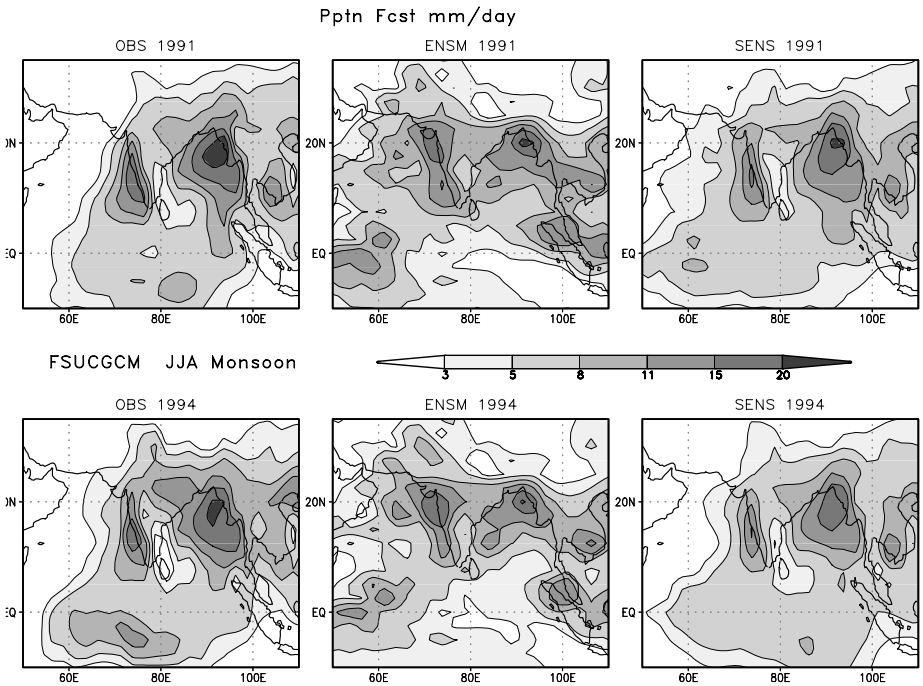

Fig. 10. An example of seasonal total precipitation forecast (mm day^{-1}) for the summer monsoon season of 1991 and 1994. The observed field is shown in the left panel (based on Xie-Arkin 1997 data sets); the middle panel shows the results from the ensemble mean of 4 FSU models and the right panel show those from the synthetic super ensemble.

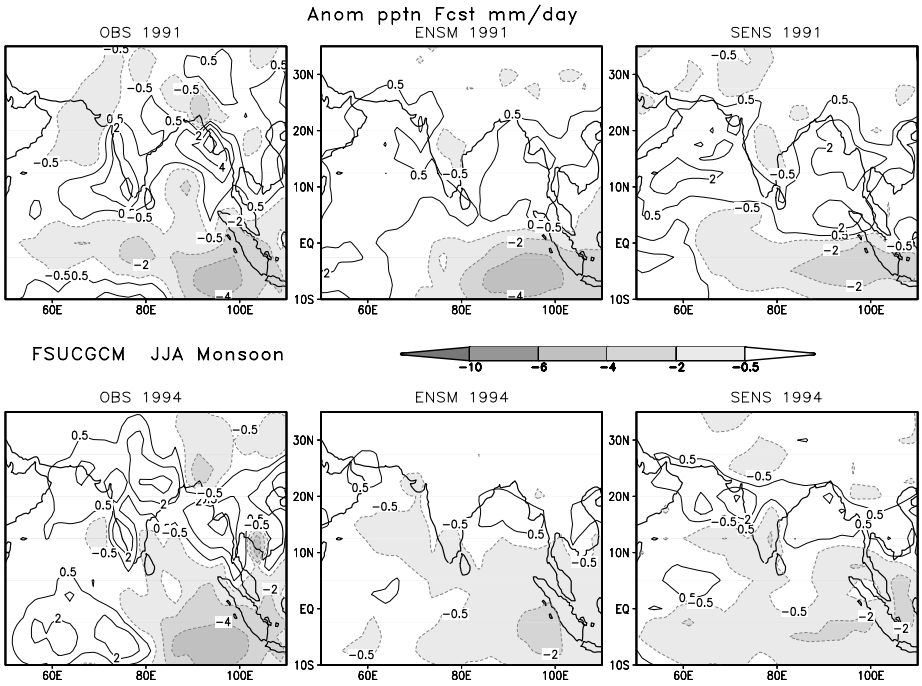

Fig. 11. Same as Figure 10 but for the precipitation anomalies.

observed anomalies. The individual member models' monsoon rainfall forecasts from the coupled suite of the present study were not very impressive as compared to the ensemble mean and the superensemble. Their RMS errors for the member models were 0.5–1.0 mm day^{-1} larger than those of the synthetic superensemble (Fig. 9c). In spite of this, much superior performance of the synthetic superensemble was noted, and the following interpretation for these skills for the total rainfall forecasts can be offered. The member models carry large systematic errors that render their scores rather low, whereas the superensembles by virtue of their ability to correct such systematic errors can perform 'better'. That 'better' may be no more than the ability of the superensemble to push its forecast towards a better climatology. If that is all that the synthetic superensemble does, then one needs to ask about the skill for the seasonal precipitation anomalies, which are central to any climate forecast. Figure 11 illustrates examples of precipitation anomaly forecasts. These anomalies are calculated with respect to the observed and the forecast seasonal mean values to define the observed or the forecast anomalies, respectively. These anomaly correlations are generally of the order of 0.2–0.5 over the monsoon domain, thus the overall skill of forecasts for the seasonal anomalies is small for these member models. Those skills were only slightly better for the synthetic superensemble. Some examples of seasonal rainfall forecast anomaly fields do seem very encouraging in that they do seem to provide some useful guidance on where to expect above or below normal monsoon rains a season in advance.

Next, some rainfall forecast examples from DEMETER and FSU coupled models are illustrated. The total seasonal precipitation forecasts for years 1999 and 2000 from the different models are shown in Figs. 12 and 13, respectively. These are examples for a relatively dry and a wet season, respectively (defined with respect to the mean values as seen in Xie-Arkin data set). During the 1999 season, there were two belts of heavy seasonal rain over the west coast of India, northern Bay of Bengal and southern Indochina. The rest of the Asian monsoon region experienced lesser rains. In Fig. 12 we show the fields of total rain during 1999. The individual models carry several different seasonal totals in their predictions for 1999. The differences between the member models' total seasonal rain and the observed total are larger than conventional anomalies that are normally projected. Among the several panels shown, the only seasonal predicted rainfall totals that closely resemble the observed counterpart for the year 1999 are from the synthetic superensemble. The ensemble mean from the suite of four FSU models capture the features for the year 1999 but the amplitudes seem to be somewhat smaller. Among the seven DEMETER models, the UKMO model (that carries the high resolution for the ocean model) captures the Bay of Bengal feature reasonably; the Arabian Sea coastal rain over India is somewhat underestimated, and it fails to capture the rainfall maxima over Indochina. Furthermore, this best model among the DEMETER suite has a belt of heavy rain into the north central India stretching from the Bay that is somewhat overestimated. A corresponding set of figures for the year 2000, a relatively wet monsoon, is shown in Fig. 13. The total rainfall for the summer season is again best predicted

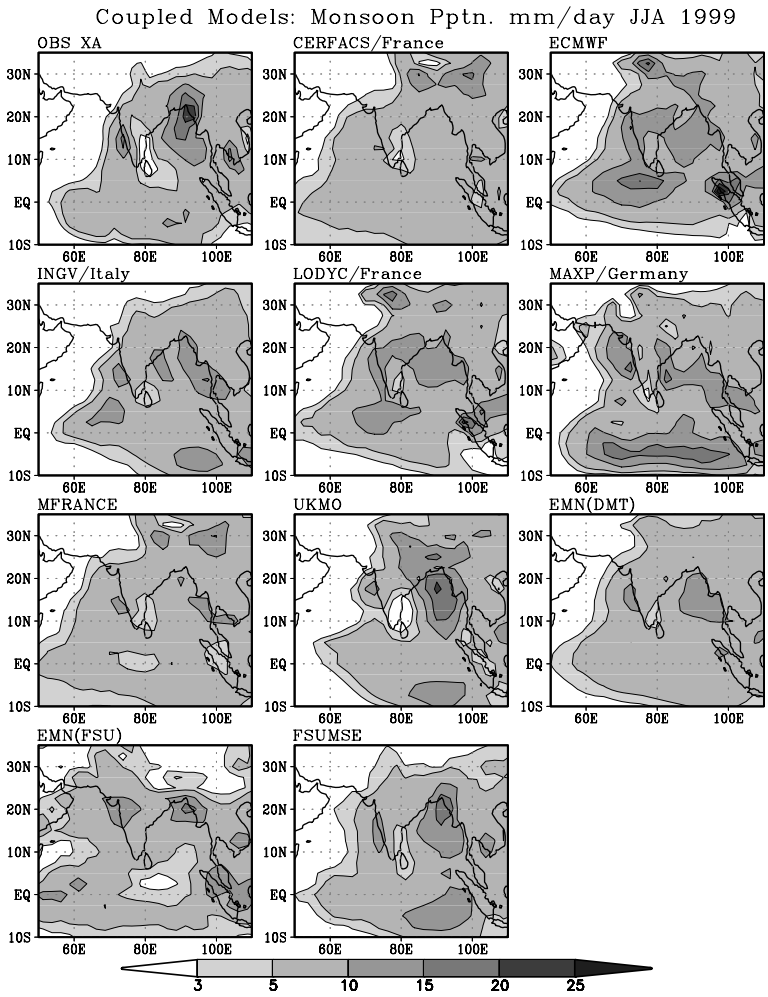

Fig. 12. An example of seasonal forecast of precipitation (mm day^{-1}) for a relatively dry monsoon year 1999 is shown. The observed estimates from Xie and Arkin (1997), from the member models of DEMETER and those from the ensemble mean of the four FSU models and those from the FSU synthetic superensemble are shown.

by the synthetic superensemble. These observed totals for the year 1999 and 2000 do look quite similar, even though one is a below normal rainfall year and the other is an above normal year. Models with poor rainfall climatology show rather large departures in the total rainfall for the season. Furthermore, these same member models exhibit large departures for their rainfall totals from one year to the next. The model climatology over the monsoon region is sensitive to many model features that contribute to such errors. These member model rainfall totals for the year 2000 depart considerably from the observed totals. Thus, it becomes a little difficult to place much credence to the member model based anomaly forecasts when they are calculated with respect to their own individual mean fields for that year. This is one of the reasons why the monsoon forecasts over seasonal time scale have been one of the most difficult areas. Some models, such as the UKMO, show excessive total rains (Fig. 13) in the interior of India over the Gangetic and Brahamputra valley regardless of whether it is a relatively dry or a wet year. The important message here is that from a construction of the synthetic superensemble, it is possible to remove such seasonal biases for seasonal forecasts of monsoon rainfall.

Figures 14 and 15 show the seasonal anomaly forecasts for the years 1999 (dry) and 2000 (wet). The observed rainfall anomalies for 1999 show a spread of negative anomalies except over northeastern India and Bangladesh. The synthetic superensemble reasonably reproduces that spread of negative anomalies. The synthetic superensemble, however, fails to capture the enhanced positive rainfall anomalies north of the Bay of Bengal over land. When the member models' performance was examined, it was noted that most of the models have failed to predict the distribution of seasonal rainfall anomalies. The ECMWF, INGV, LODYC, UKMO and other DEMETER models predict strong positive anomalies, that is, above normal rain, over most of northern India during this season when below normal rains were observed. Given this spread, it is possible to correct these biases from the construction of synthetic superensemble, which was also superior to the ensemble mean for the precipitation anomalies. The observed anomaly for the year 2000 (a wet year

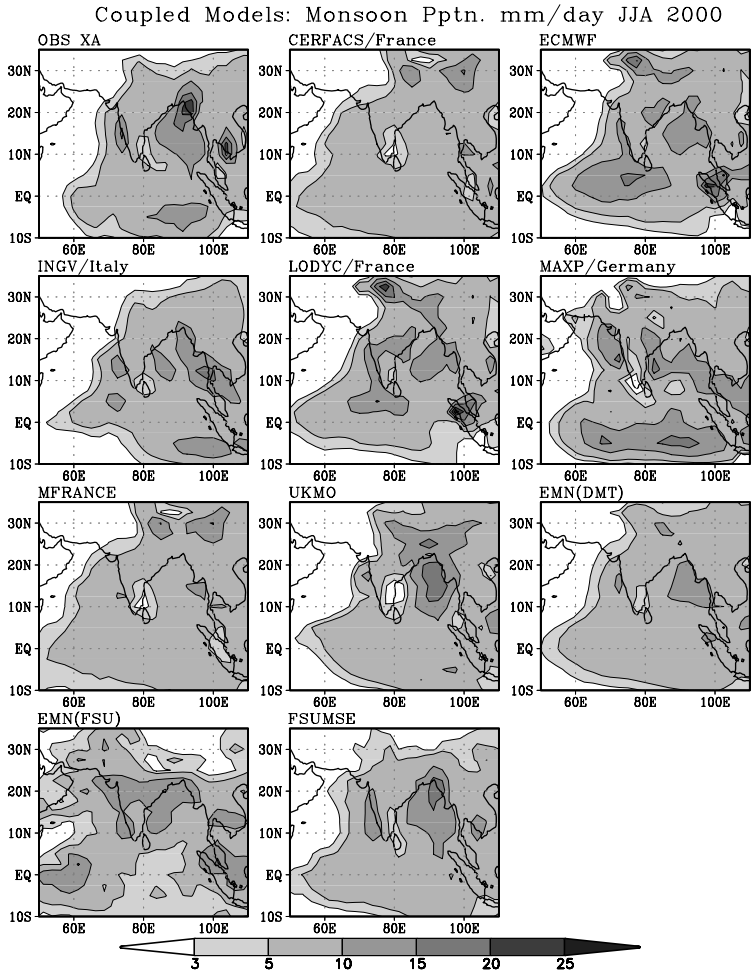

Fig. 13. Same as Figure 12 except that those pertain to a relatively wet monsoon year 2000.

over central/peninsular India and southern Indochina) carries an alternating (west to east) anomaly pattern. Below normal values over the central Arabian Sea, a wet area over central/peninsular India, a below normal anomaly over the northern Bay of Bengal, and a wet anomaly over southern Indochina are seen in these observed fields. The synthetic superensemble reasonably reproduces these features. Among the DEMETER models, the alternating (west to east) pattern was only seen for the LODYC model of France and the UKMO coupled model. These two did capture the general features quite well, although the northern India rainfall had a somewhat excessive spread of heavy rains, which was also reflected in the UKMO model forecasts. The ensemble mean (bottom left panel) does not capture the below normal rain over the central Arabian Sea. Overall, the synthetic superensemble seems to carry the seasonal forecasts of these wet and dry spells somewhat better than the member models and the ensemble mean.

To examine the probabilistic skills of the superensemble forecasts, the Brier Skill Score was computed, which is a measure of the improvement of a probabilistic forecast relative to a climatological forecast. Ideally, a forecast for X% probability of a certain event (e.g. precipitation exceeding a given threshold) would verify X% of times. Figures 16(a)–(c) illustrates the observed frequency vs. the forecast probability of precipitation anomaly (over the monsoon domain) exceeding 1, 2 and 3 mm day^{-1}. The ensemble mean (denoted by EM) tends to systematically overestimate the probability of events, while the superensemble (denoted by SSE) and the synthetic ensemble mean (denoted by SEM) tend to be somewhat underestimating it. The reliability (measured by the closeness of the forecasts to the 45 degree line) of the superensemble and the synthetic ensemble mean is higher than that of the ensemble mean. The Brier Skill Score accounts for both the reliability and the resolution of probabilistic forecasts (the latter being the ability of the forecasts to correctly produce probabilistic forecasts away from the climatological probability). The overall skill score of both superensemble and synthetic ensemble is higher than that of the ensemble for most thresholds, with the amount of improvement increasing with increase of the threshold value (Fig. 16d).

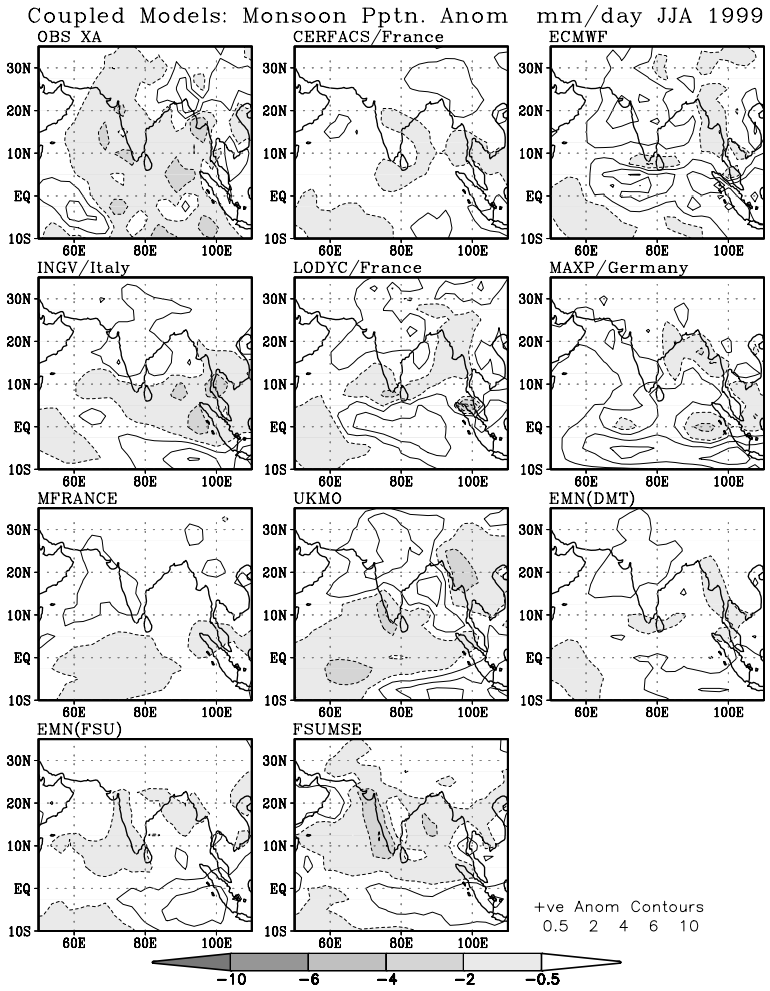

Fig. 14. Seasonal precipitation anomaly for a relatively dry year 1999, units mm day^{-1}; Top left: Observed estimates based on Xie and Arkin (1997). Bottom Panels: (left) Forecasts from the ensemble mean of the FSU models, (right) Forecasts from the FSU synthetic superensemble, other panels show forecasts from the European DEMETER models.

6.2. Seasonal predictions of SSTs and surface air temperatures

From the suite of four FSU coupled models we archived the SSTs and the predicted land surface temperatures. The DEMETER database that was provided to us by ECMWF did not include the SST fields; instead, they provided air temperature at the 2 m level. We have constructed two separate synthetic superensembles from these respective data sets (one for SSTs and one for 2-m air temperatures). That exercise based on the total data sets, described in section 2, was very worthwhile. Figures 17a and b show the RMS and the anomaly correlation from these two databases (FSU and DEMETER), respectively. These cover the regions of the tropics between 30°S to 30°N. The results in both cases are most striking. The RMS errors of the SSTA and surface air temperatures are both drastically reduced from values around 4° to 5° C (for the member models) to 1° C (for the synthetic superensemble) and, for surface air temperature, from values around 1 to 2° C to 0.5° C for the DEMETER models. This shows that the synthetic superensemble is a powerful tool for handling of the SSTA and the surface air temperature forecasts. It is also interesting to note that RMS errors of the synthetic superensemble do not show any marked variations in skill during the transition from an El Niño to a La Niña year, of which several were present during the years covered by our forecast phase. Given such improvements in the SSTA and air temperature's seasonal forecasts it should be possible to improve the forecasts of air sea interaction, that is, the surface fluxes from this product. The inset panels on the far right of each diagram (Fig. 17) show the summary for the 15 yr of forecast, which clearly indicates an overall marked reduction of RMS errors. The anomaly correlations of these fields were also calculated and some improvements from the synthetic superensemble were noted. The member model values were around 0.4 and were raised to the level 0.5 for the synthetic superensemble for both the SST and land surface temperature data sets from the FSU coupled model forecasts and for the 2 m temperatures of the DEMETER. Some examples of field distributions of the SST (based on the FSU coupled model) and of the surface air temperatures based on the DEMETER data sets are presented in

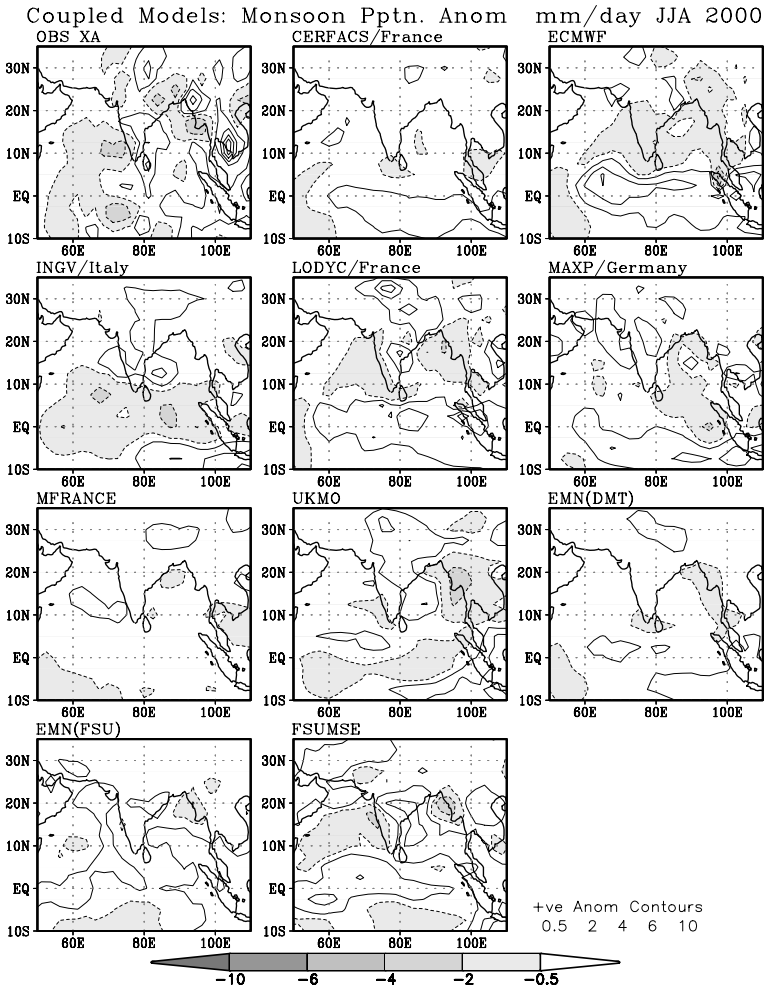

Fig. 15. Same as Figure 14 but for the year 2000, a relatively wet year.

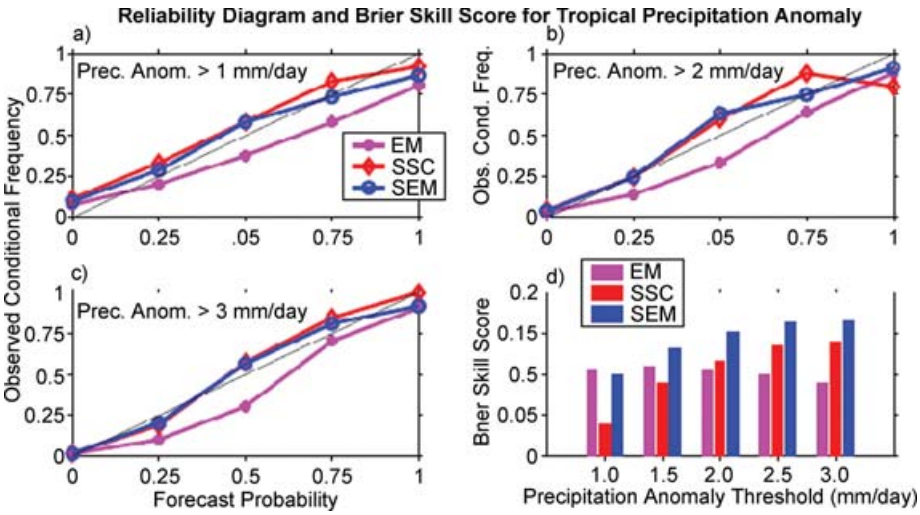

Fig. 16. Probabilistic skill scores for precipitation anomaly forecasts for ensemble mean (EM), synthetic ensemble mean (SEM) and synthetic superensemble (SSE). Panels (a), (b), and (c) illustrate the forecast probability against observed relative frequency of occurrence for different thresholds of precipitation anomalies at >1, > 2, and >3 mm day^{-1}, respectively. Panel (d) summarizes the Brier Skill Scores at different thresholds of precipitation anomalies.

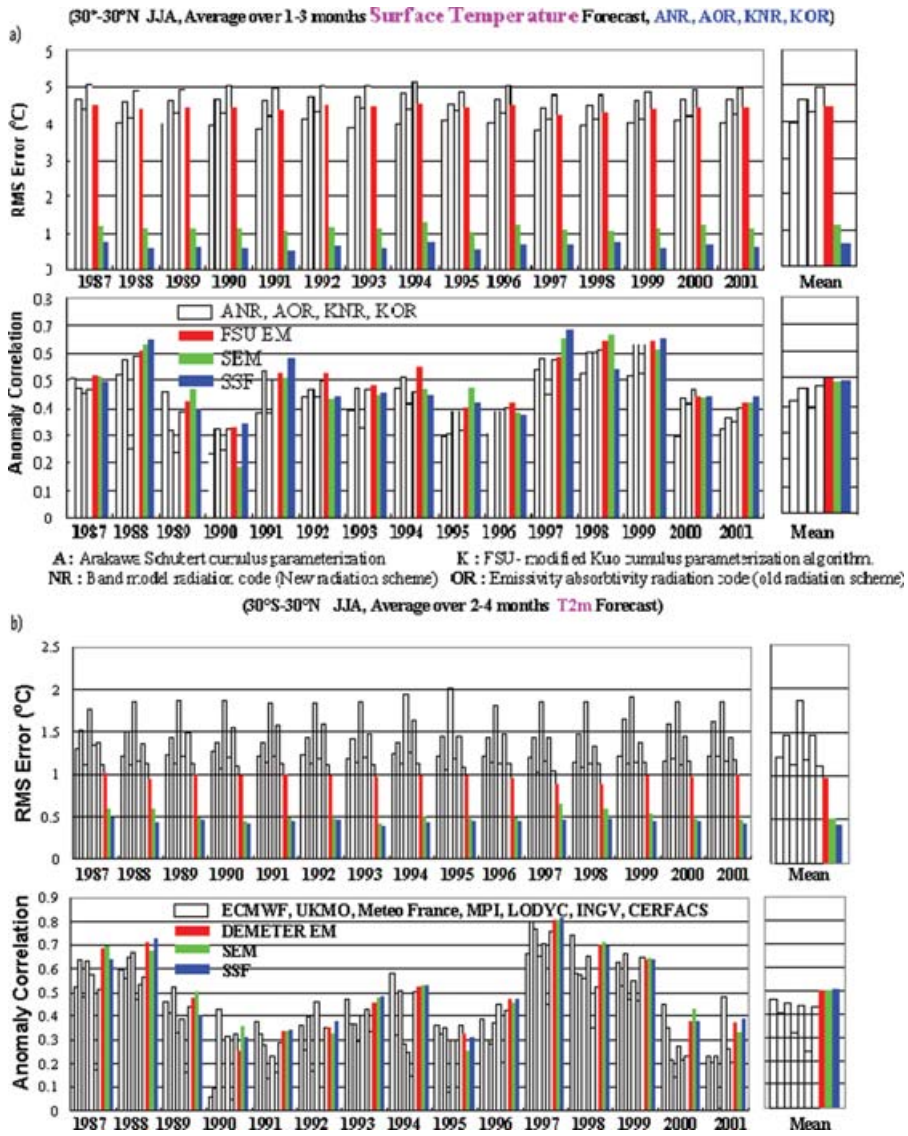

Fig. 17. (a) Observed and predicted fields of SST and surface temperature over land (units K). In sequence top to bottom: Observed fields based on Reynolds SST over ocean and ECMWF nowcasting over land; the ensemble mean from FSU models; the synthetic ensemble mean from FSU models and the synthetic superensemble of FSU models; (b) Same as (a) except for 2 m air temperature based on the seven DEMETER models.

Figs. 18 and 19, respectively. In sequence, the 4 panels of these two figures include 'observed' fields based on Reynolds SST fields (Reynolds and Smith, 1994) and the ECMWF analysis of the surface air temperatures, the ensemble mean of the forecasts from the four models, the synthetic ensemble mean, and the synthetic superensemble based forecasts. A comparison of these forecasts with the 'observed' counterparts clearly shows that the synthetic superensemble based forecast fields are indeed very close to the observed fields. In contrast, the conventional ensemble mean of the base models do show some marked errors. The synthetic ensemble mean appears to be a superior product and very promising for seasonal forecasts of SST and surface air temperatures.

7. Concluding remarks

The biggest contribution of this study was in the drastic reduction of RMS error and a slight improvement for the anomaly correlation for seasonal forecasts of the monsoon. The participating models in this superensemble exercise included all of the best available coupled atmosphere–ocean models from Europe and a suite of FSU models. This study utilizes no less than a total of 4500 seasonal climate forecasts from these models. This is one of the largest collections of data sets for seasonal climate forecasts. The synthetic superensemble used in this study is based on an equal number of proxy seasonal forecasts where observed structures based on principal component time series and empirical

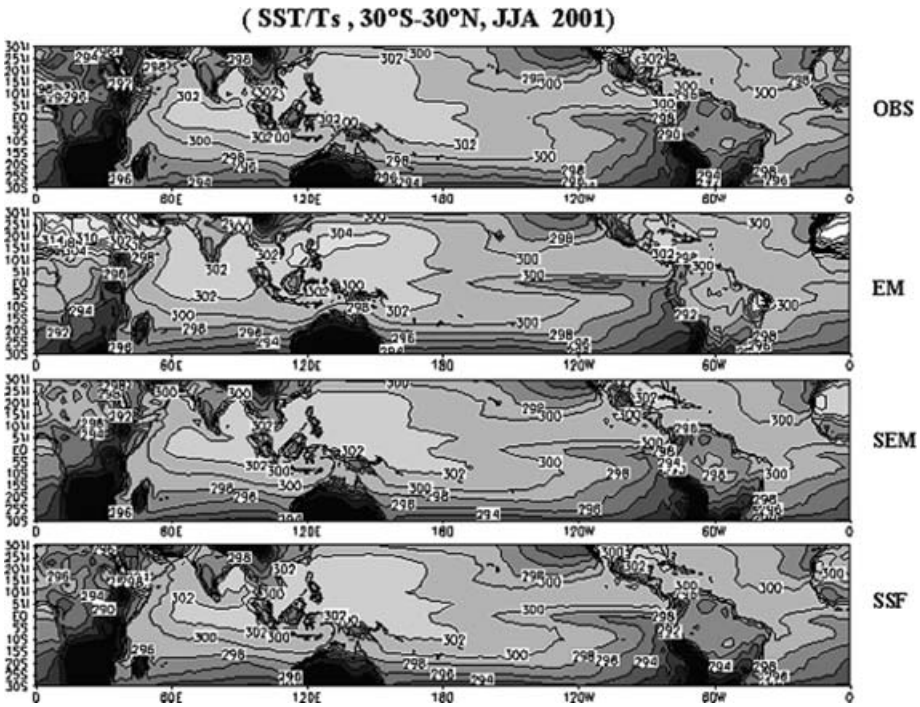

Fig. 18. Observed and predicted fields of SST and surface temperature over land (units K). In sequence top to bottom: Observed fields based on Reynolds SST over ocean and ECMWF nowcasting over land; the ensemble mean from FSU models; the synthetic ensemble mean from FSU models and the synthetic superensemble of FSU models.

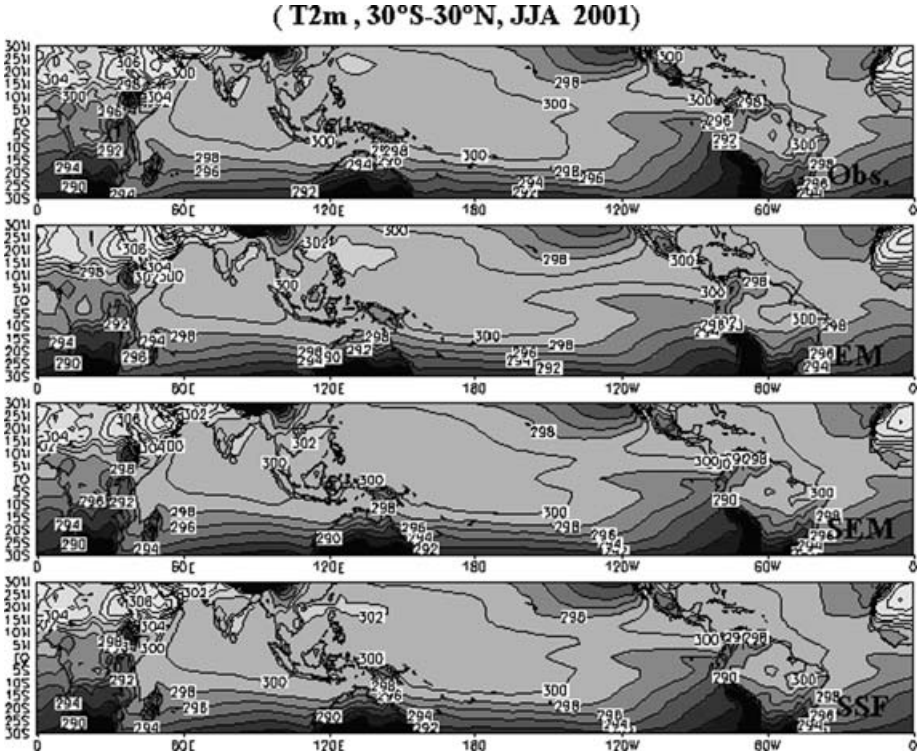

Fig. 19. Same as Figure 18 except for 2 m air temperature based on the seven DEMETER models.

orthogonal functions were projected on to the forecast components for each model run. The superensemble combines multimodel forecast runs to arrive at an improved product that easily outperforms the participating member models. This product is also clearly better than an ensemble mean of the participating models. The suite of FSU coupled models deployed for this synthetic superensemble was first independently studied to assess its integrity for simulating seasonal mean climatological features and the monsoon. We noted that the overall performances of these individual FSU models are comparable to the best among the European suite of models (DEMETER). It was possible to demonstrate seasonal simulation for fields such as precipitation, SST and surface air temperatures.

The construction of a superensemble seemed worthwhile. The skills are much improved compared to those of the member coupled models. The higher skills for the synthetic superensemble seem to arise because of two reasons: the PC time series and the EOF selection (roughly 55 modes) do seem to filter out some of the higher frequency noise from the full field that degrades the skills somewhat. The spatial structures (EOFs) for model forecasts are projected based on the observed part of the training phase. The time evolution of the seasonal anomalies in model forecasts are handled better due to the use of weights determined from the statistics of principal component time series data of models and the observational counterpart during the training phase. The final superensemble weights are determined from synthetic data sets thus constructed.

In this study, our main focus is on the issues of investigating the quality of simulation/ forecast from the coupled models. We looked at the quality of precipitation hindcasts from DEMETER as well as the FSU coupled models. The development and testing of 'Synthetic Superensemble Method' with FSU coupled model data paved the way to employ the same procedure for the DEMETER data sets, where we examined if we could improve upon the simple 'Ensemble Mean'. We are aware of the complexity of the issue of dynamical seasonal monsoon forecasting. Forecasting seasonal climate of monsoon by coupled models has just begun in recent years. We have no intention of comparing DEMETER with FSU, but as the data were available, we got an opportunity to look at the simulation quality.

Tropical and monsoon precipitation skills (RMS errors) for seasonal forecasts show that member model skills are almost two times lower compared to those of the synthetic superensemble. The superensemble is designed for a least square minimization of the RMS error. Thus, the result is not surprising. The expression for the anomaly correlation entails products of domain sums and is not that straightforward and amenable to improvement using a minimization principle. There are improvements in the anomaly correlations of global and monsoon precipitation forecasts (over the seasonal time scale); the anomaly correlations for the synthetic superensemble are indeed higher than those of the member models and their member mean. That increase of anomaly correlation (over the best model) is only of the order of 0.1 and 0.2. In this study, we have also examined the RMS and anomaly correlation forecast skills for several other variables over the entire tropical belt between 30°S and 30°N and the South Asian monsoon region and found similar improvements. The probabilistic skill (Brier Skill Score) computations also revealed enhanced performance by the synthetic superensemble compared to the ensemble mean and the member models. The synthetic superensemble approach thus has the potential to give better results for seasonal climate forecasts for the monsoon region, and can provide useful guidance.

Acknowledgments

We gratefully acknowledge, the ECMWF for providing observed analysis and seven DEMETER coupled model data sets. The research reported here was supported by NSF grant number ATM-0108741, NOAA grant number NA06GPO512, FSURF grant number 1338-831-45, and NASA grants NAG5-13563.

References

Anderson, D. 1999. Extremes in the Indian Ocean. *Nature* **401**, 337–338

Ashok, K., Guan, Z. and Yamagata, T. 2001. Influence of the Indian Ocean Dipole on the relationship between the Indian monsoon rainfall and ENSO. *Geophys. Res. Lett.* **28**, 4499–4502.

Ashok, K., Guan, Z., Saji, N. H. and Yamagata, T. 2004. Individual and combined influences of ENSO and the IOD on the Indian summer monsoon. *J. Climate* **17**, 3141–3155.

Barnett, T. P. 1983. Interaction of the monsoon and Pacific trade wind system at interannual time scales. Part I: the equatorial zone. *Mon. Wea. Rev.* **111**, 756–773.

Behera, S. K., Krishnan, R. and Yamagata, T. 1999. Unusual ocean-atmosphere conditions in the tropical Indian Ocean during 1994. *Geophys. Res. Lett.* **26**, 3001–3004.

Chang, C. B. 1979. On the influence of solar radiation and diurnal variation of surface temperatures on African Disturbances, Repp. 79-3. Dept. of Meteorology, Florida State University, Tallahassee, Fl 32306, p. 157.

Douville, H. 2002. Influence of soil moisture on the Asian and African Monsoons. Part II: interannual variability. *J. Climate* **15**, 701–720.

Douville, H., Chauvin, F. and Broqua, H. 2001. Influence of soil moisture on the Asian and African monsoons. Part I: mean monsoon and daily precipitation. *J. Climate* **14**, 2381–2403.

Fu, X., Wang, B. and Li, T. 2002. Impacts of air–sea coupling on the simulation of mean Asian summer monsoon in the ECHAM4 Model. *Mon. Wea. Rev.* **130**, 2889–2904.

Gadgil, S. and Sajani, S. 1998. Monsoon precipitations in AMIP runs. *Clim. Dyn.* **14**, 659–689.

Gadgil, S., Vinayachandran, P. N. and Francis, P. A. 2003. Droughts of the Indian summer monsoon: Role of clouds over the Indian Ocean. *Curr. Sc.* **85**, 1713–1720.

Gates, W. L., Boyle, J. S., Covey, C., Dease, C. G., Doutriaux, C. M., and co-authors. 1999. An overview of the results of the Atmospheric Model Intercomparison Project (AMIP I). *Bull. Amer. Meteor. Soc.* **80**, 29–55.

Grell, G. A. 1993. Prognostic evaluation of assumptions used by cumulus parameterization. *Mon. Wea. Rev.* **121**, 764–787.

Inness, P. M. and Slingo, J. M. 2003. Simulation of the Madden–Julian oscillation in a coupled general circulation model. Part I: comparison

with observations and an atmosphere-only GCM. *J. Climate* **16**, 345–364.

Ji, Y. and Vernekar, A. D. 1997. Simulations of the Asian summer monsoons of 1987 and 1988 with a regional model nested in a global GCM. *J. Climate* **10**, 1965–1979.

Kang, I.-S., Jin, K., Wang, B., Lau, K.-M., Shukla, J., and co-authors. 2002. Intercomparison of the climatological variations of Asian summer monsoon precipitation simulated by 10 GCMs. *Clim. Dyn.* **19**, 383–395.

Kemball, C. S., Wang, B. and Fu, X. 2002. Simulation of the ISO in the ECHAM4 model: the impact of coupling with an ocean model. *J Atmos. Sci.* **59**, 1433–1453

Krishnamurti, T. N. and Bedi, H. S. 1988. Cumulus Parameterization and rainfall rates-3. *Mon. Wea. Rev.* **116**, 583–599.

Krishnamurti, T. N., Xue, J., Bedi, H. S., Ingles, K. and Oosterhof, D. 1991. Physical Initialization for Numerical Weather Prediction over the Tropics. *Tellus* **43AB**, 53–81.

Krishnamurti, T. N., Bedi, H. S. and Hardiker, V. 1998. *Introduction to Global Spectral Modeling*. Oxford University Press, New York, 253 pp.

Krishnamurti, T. N., Kishtawal, C. M., LaRow, T. E., Bachiochi, D. R., Zhang, Z., and co-authors. 1999. Improved weather and seasonal climate forecasts from multimodel superensemble. *Science* **285**, 1548–1550

Krishnamurti, T. N., Kishtawal, C. M., Zhang, Z., LaRow, T., Bachiochi, D., and co-authors. 2000a. Multimodel ensemble forecasts for weather and seasonal climate. *J. Climate* **13**, 4196–4216.

Krishnamurti, T. N., Bachiochi, D., LaRow, T., Jha, B., Tewari, M. and co-authors. 2000b. Coupled atmosphere-ocean modeling of El Niño of 1997–98. *J. Clim.* **13**, 2428–2459.

Krishnamurti, T. N., Stefanova, L., Chakraborty, A., Kumar, T. S. V. V., Cocke S., and co-authors. 2002. Seasonal forecasts of precipitation anomalies for North American and Asian monsoons. *J. Met. Soc. Japan* **80**, 1415–1426

Krishnamurti, T. N., Chakraborty, D. R., Cubukcu, N., Stefanova, L. and Kumar, T. S. V. V. 2003. A mechanism of the Madden–Julian Oscillation based on interactions in the frequency domain. *Quart. J. Royal Met. Soc.* **129**, 2559–2590.

Krishnamurti, T. N. and Vijay Kumar, T. S. V. 2004. Superensemble forecasts for weather and climate. *Proc. of Ind. National Sci. Acad.* **69A**, 567–583.

Lacis, A. A. and Hansen, J. E. 1974. A parameterization for absorption of solar radiation in the Earth's atmosphere. *J. Atmos. Sci.* **31**, 118–133

LaRow, T. E. and Krishnamurti, T. N. 1998. Seasonal prediction using a coupled ocean-atmosphere model with data assimilation. *Tellus* **50A**, 76–94.

Latif, M. 1987. Tropical ocean circulation experiments. *J. Phys. Oceanogr.* **17**, 246–263

Lau, N. C. and Nath, M. J. 2003. Atmosphere-Ocean variations in the Indo-Pacific sector during ENSO episodes. *J. Clim.* **16**, 3–20.

Lau, N. C. and Nath, M. J. 2004. Coupled GCM simulation of atmosphere-ocean variability associated with zonally asymmetric SST changes in the tropical Indian Ocean. *J. Clim.* **17**, 245–265.

Molteni, F., Corti, S., Ferranti, L. and Slingo, J. M. 2003. Predictability Experiments for the Asian summer monsoon: impact of SST anomalies on interannual and intraseasonal variability. *J. Clim.* **16**, 4001–4021.

Murtugudde, R., McCreary, J. P. and Busalacchi, A. J. 2000. Oceanic processes associated with anomalous events in the Indian Ocean with relevance to 1997–1998. *J. Geophys. Res.* **C2 105**, 3295–3306.

Palmer, T. N. and co-authors 2004. Development of a European Multi-Model Ensemble System for Seasonal to Inter-Annual Prediction (DEMETER). *Bull. Amer. Met. Soc.* **85**, 853–872.

Rasmusson, E. M. and Carpenter, T. H. 1983. The relationship between eastern equatorial Pacific sea surface temperatures and rainfall over India and Sri Lanka. *Mon. Wea. Rev.* **110**, 517–528.

Rao, S. A., Behera, S. K., Masumoto, Y. and Yamagata, T. 2002. Interannual subsurface variability in the tropical Indian Ocean with a special emphasis on the Indian Ocean Dipole. *Deep- Sea Res II* **49**, 1549–1572

Rao, D. V. B., Ashok, K. and Yamagata, T. 2004. A numerical simulation study of the Indian summer monsoon of 1994 using NCAR MM5. *J. Met. Soc. Japan* **82**, 1755–1775.

Reynolds, R. W. and Smith, T. M. 1994. Improved global SST analysis using O. I. *J. Climate* **7**, 929–948.

Saji, N. H., Goswami, B. N., Vinyachandran, P. N. and Yamagata, T. 1999. A dipole mode in the tropical Indian Ocean. *Nature* **401**, 360–363.

Schubert, S. D. and Wu, M. L. 2001. Predictability of the 1997 and 1998 South Asian Summer Monsoon Low-Level Winds. *J. Clim.* **14**, 3173–3191.

Shen, X., Kimoto, M. and Sumi, A. 1998. Role of land surface processes associated with interannual variability of broad scale Asian summer monsoon as simulated by the CCSR/NIES AGCM. *J. Met. Soc. Japan* **76**, 217–236.

Slingo, J. M. and Annamalai, H. 2000. 1997: The El Niño of the century and the response of the Indian Summer Monsoon. *Mon. Wea. Rev.* **128**, 1778–1797.

Sperber, K. R. and Palmer, T. N. 1996. Interannual tropical rainfall variability in a GCM simulation associated with the AMIP. *J. Climate* **9**, 2727–2750.

Sperber, K. R., Brankovic, C., Deque, M., Frederiksen, C. S., Graham, R., and co-authors. 2001. Dynamical seasonal predictability of the Asian summer monsoon. *Mon. Wea. Rev.* **129**, 2226–2248.

Stefanova, L. and Krishnamurti, T. N. 2002. Interpretation of seasonal climate forecast using Brier skill score. *J. Clim.* **15**, 537–544.

Vinayachandran, P. N., Iizuka, S. and Yamagata, T. 2002. Indian Ocean dipole mode event in an ocean general circulation model. *Deep-Sea Res II,* **49**, 1573–1596

Wang, B., Kang, I.-S. and Lee, J.-Y. 2004. Ensemble simulations of Asian–Australian monsoon variability by 11 AGCMs. *J. Climate* **17**, 803–818.

Webster, P. J., Moore, A. M., Loschingg, J. P. and Leben, R. R. 1999. Coupled ocean-atmosphere dynamics in the Indian Ocean during 1997–98. *Nature* **401**, 356–360.

Wu, M. L. C., Schubert, S., Kang, I.-S. and Waliser, D. E. 2002. Forced and free intraseasonal variability over the South Asian monsoon region simulated by 10 AGCMs. *J. Clim.* **15**, 2862–2880.

Xie, P. and Arkin, P. A. 1997. Global precipitation: a 17 year monthly analysis based on observations, satellite estimates and numerical model outputs. *Bull. Amer. Met. Soc.* **78**, 2539–2558.

Yun, W. T., Stefanova, L., Mitra, A. K., Kumar, T. S. V. V., Dewar, W. and co-authors. 2005. Multimodel synthetic superensemble algorithm for seasonal climate prediction using DEMETER forecasts. *Tellus* **57A**, 280–289.